ARTICLES

Tankyrase inhibition stabilizes axin and antagonizes Wnt signalling

Shih-Min A. Huang[1], Yuji M. Mishina[1], Shanming Liu[1], Atwood Cheung[1], Frank Stegmeier[1], Gregory A. Michaud[1], Olga Charlat[1], Elizabeth Wiellette[1], Yue Zhang[1], Stephanie Wiessner[1], Marc Hild[1], Xiaoying Shi[1], Christopher J. Wilson[1], Craig Mickanin[1], Vic Myer[1], Aleem Fazal[1], Ronald Tomlinson[1], Fabrizio Serluca[1], Wenlin Shao[1], Hong Cheng[1], Michael Shultz[1], Christina Rau[2], Markus Schirle[2]†, Judith Schlegl[2], Sonja Ghidelli[2], Stephen Fawell[1], Chris Lu[1], Daniel Curtis[1], Marc W. Kirschner[3], Christoph Lengauer[1]†, Peter M. Finan[1], John A. Tallarico[1], Tewis Bouwmeester[2]†, Jeffery A. Porter[1], Andreas Bauer[2]† & Feng Cong[1]

The stability of the Wnt pathway transcription factor β-catenin is tightly regulated by the multi-subunit destruction complex. Deregulated Wnt pathway activity has been implicated in many cancers, making this pathway an attractive target for anticancer therapies. However, the development of targeted Wnt pathway inhibitors has been hampered by the limited number of pathway components that are amenable to small molecule inhibition. Here, we used a chemical genetic screen to identify a small molecule, XAV939, which selectively inhibits β-catenin-mediated transcription. XAV939 stimulates β-catenin degradation by stabilizing axin, the concentration-limiting component of the destruction complex. Using a quantitative chemical proteomic approach, we discovered that XAV939 stabilizes axin by inhibiting the poly-ADP-ribosylating enzymes tankyrase 1 and tankyrase 2. Both tankyrase isoforms interact with a highly conserved domain of axin and stimulate its degradation through the ubiquitin-proteasome pathway. Thus, our study provides new mechanistic insights into the regulation of axin protein homeostasis and presents new avenues for targeted Wnt pathway therapies.

The evolutionarily conserved Wnt/β-catenin signal transduction pathway controls many biological processes[1]. A key feature of the Wnt pathway is the regulated proteolysis of the downstream effector β-catenin by the β-catenin destruction complex. The principal constituents of the β-catenin destruction complex are adenomatous polyposis coli (APC), axin and glycogen synthase kinase 3α/β (GSK3α/β). In the absence of Wnt pathway activation, cytosolic β-catenin is constitutively phosphorylated and targeted for degradation. On Wnt stimulation the β-catenin destruction complex dissociates, leading to the accumulation of nuclear β-catenin and transcription of Wnt pathway-responsive genes.

Inappropriate activation of the Wnt pathway has been observed in many cancers[2,3]. Notably, truncating mutations of the tumour suppressor APC are the most prevalent genetic alterations in colorectal carcinomas[4–6]. The efficient assembly of the multi-protein destruction complex is dependent on the steady-state levels of its principal constituents. Axin has been reported to be the concentration-limiting factor in regulating the efficiency of the β-catenin destruction complex[7,8] and overexpression of axin induces β-catenin degradation in cell lines expressing truncated APC[9–11]. Thus, it is likely that axin protein levels need to be tightly regulated to ensure proper Wnt pathway signalling. In fact, Wnt signalling itself regulates the level of axin at several steps, with *AXIN2* being a major transcriptional target of the β-catenin–T-cell factor (TCF) complex and Wnt signalling promoting the degradation of axin[12,13]. However, the molecular mechanisms that regulate protein homeostasis of destruction complex components and complex assembly remain elusive.

In this study we used chemical-genetic and -proteomic approaches to search for novel modulators of the Wnt signalling pathway. We identified a low molecular mass compound that can prolong the half-life of axin and promote β-catenin degradation through inhibiting tankyrase (TNKS). Our study uncovers a new mechanism that controls axin protein stability and Wnt pathway signalling, and its therapeutic exploitation holds promise for treating Wnt-pathway-dependent cancers.

XAV939 inhibits Wnt signalling by increasing axin levels

XAV939 was identified as a small molecule inhibitor of the Wnt/β-catenin pathway from a high-throughput screen using a Wnt-responsive Super-Topflash (STF) luciferase reporter assay in HEK293 cells (Fig. 1a). XAV939 strongly inhibited Wnt3a-stimulated STF activity in HEK293 cells, but did not affect CRE, NF-κB or TGF-β luciferase reporters (Fig. 1b). In contrast, LDW643, a close structural analogue of XAV939 (Fig. 1a), had no effect on the Wnt3a-induced STF reporter (Fig. 1b). XAV939 treatment blocked Wnt3a-induced accumulation of β-catenin in HEK293 cells (Fig. 1c), indicating that the compound modulates Wnt signalling upstream of β-catenin. Interestingly, XAV939 also inhibited STF activity in SW480 cells, a colorectal cancer cell line harbouring a truncated APC (Fig. 1d). XAV939 decreased β-catenin abundance, but significantly increased β-catenin phosphorylation (S33/S37/T41) in SW480 cells (Fig. 1e), indicating that XAV939 promotes the phosphorylation-dependent degradation of β-catenin by increasing the activity of the destruction complex.

To explore how XAV939 may increase the activity of the destruction complex, we investigated whether compound treatment alters the protein levels of known Wnt pathway components. Notably, the

[1]Novartis Institutes for Biomedical Research, 250 Massachusetts Avenue, Cambridge, Massachusetts 02139, USA. [2]Cellzome AG, Meyerhofstrasse 1, D-69117 Heidelberg, Germany. [3]Department of Systems Biology, Harvard Medical School, Boston, Massachusetts 02115, USA. †Present addresses: Novartis Institutes for Biomedical Research, CH-4002 Basel, Switzerland (T.B., A.B.); Novartis Institutes for Biomedical Research, Cambridge, Massachusetts 02139, USA (M. Sc.); Sanofi-Aventis, 94403 Vitry-sur-Seine, France (C.L.).

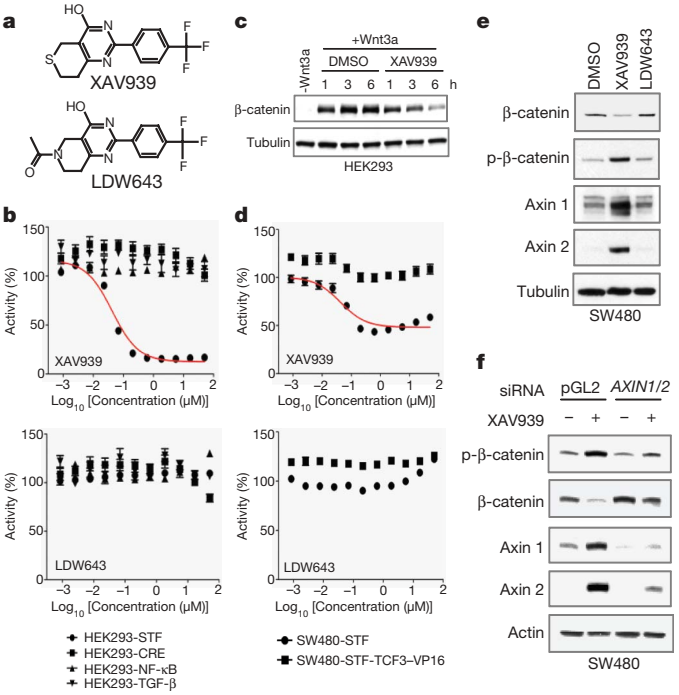

Figure 1 | XAV939 inhibits Wnt/β-catenin signalling by increasing axin protein levels. **a**, Compound structures of XAV939 and LDW643. **b**, XAV939 (24 h) specifically inhibits STF reporter, but not CRE, NF-κB or TGF-β reporter in HEK293 cells ($n = 12$). The corresponding reporter activity was normalized to DMSO. Error bars represent s.d. here and throughout the study. **c**, XAV939 (1 μM) reduces Wnt3a-induced stabilization of β-catenin in HEK293 cells. **d**, XAV939 (24 h) inhibits STF activity in APC-deficient SW480 cells ($n = 12$). SW480 cells expressing TCF3–VP16 were used as a control as overexpression of TCF3–VP16 fusion protein largely bypassed the requirement of β-catenin on STF activity. **e**, XAV939 (1 μM, 16 h) decreases the abundance of β-catenin and increases the abundance of axin and phospho-β-catenin (p-β-catenin) in SW480 cells. **f**, The effect of XAV939 on β-catenin in SW480 cells is eliminated by *AXIN1/2* siRNAs.

protein, but not messenger RNA, levels of axin 1 and axin 2 were strongly increased after XAV939 treatment (Fig. 1e and data not shown; Supplementary Fig. 1a). In addition, we noted a strong increase in axin–GSK3β complex formation, presumably because of increased axin protein levels (Supplementary Fig. 1b). Similar effects of XAV939 were also observed in DLD-1 cells, another colorectal cancer cell line with truncated APC (Supplementary Fig. 1c, d). Importantly, short interfering RNA (siRNA)-mediated depletion of axin 1/2 in SW480 cells reversed the effect of XAV939 on β-catenin degradation (Fig. 1f and Supplementary Fig. 1f) and diminished the inhibitory activity of XAV939 on the STF reporter (Supplementary Fig. 1e), indicating that XAV939 inhibits Wnt signalling by increasing axin 1/2 protein levels. Together, these findings support the hypothesis that XAV939 increases the concentration of axin–GSK3β complex, thereby promoting phosphorylation and degradation of β-catenin.

XAV939 regulates axin levels through tankyrase inhibition

To identify the cellular efficacy target(s) through which XAV939 upregulates axin protein levels, we used a three-channel iTRAQ quantitative chemical proteomics approach. This strategy is based on the immobilization of a bioactive analogue of XAV939 (Supplementary Fig. 2) to affinity-capture cellular proteins from HEK293 cell lysates spiked with an excess amount (20 μM) of XAV939, the inactive analogue LDW643 or DMSO. Specific binding to the immobilized compound should be competed with XAV939, but not with LDW643. Of 699 proteins quantified (Supplementary Table 1), 18 proteins were significantly and specifically competed-off (>65%, >2σ of the mean) with soluble XAV939 (Fig. 2a), including the poly(ADP-ribose) polymerases PARP1, PARP2, TNKS1, TNKS2 and several known PARP1 substrates, presumably co-purified with PARP1.

To establish the affinity of binding to the identified PARP proteins, we performed a compound competition experiment, and showed that XAV939, but not LDW643, blocks TNKS binding at 0.1 μM and blocks PARP1/2 binding at 1 μM (Fig. 2b). We further characterized the compound binding using Cy5-labelled XAV939 and recombinant PARP proteins. We found that XAV939 binds tightly to the catalytic (PARP) domains of TNKS1 and TNKS2 ($K_d = 0.099$ and 0.093 μM, respectively) (Fig. 2c). XAV939 also binds to recombinant PARP1, although with a significantly lower binding affinity ($K_d = 1.2$ μM).

To determine which PARP family member(s) are the actual efficacy targets of XAV939, we assessed their siRNA-mediated loss-of-function phenotypes. Co-depletion of TNKS1 and TNKS2 phenocopied the effect of XAV939 by increasing the protein levels of axin 1 and 2, whereas combinatorial *PARP1/2* knockdown did not (Fig. 3a and Supplementary Fig. 3a, b). In addition, ABT-888, a potent PARP1 and PARP2 inhibitor[14] that has minimal activity on TNKS1 and

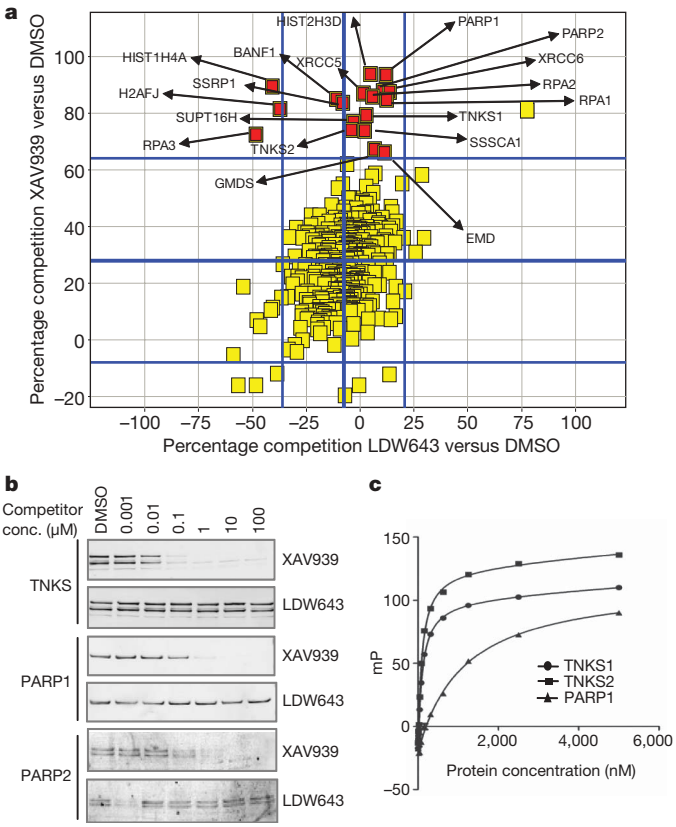

Figure 2 | Identification of the cellular efficacy targets of XAV939. **a**, Scatter plot depicting all proteins ($n = 398$) identified and quantified with >3 unique spectra in a three-channel iTRAQ quantitative chemical proteomics experiment. Proteins are plotted as a function of the percentage competition with the active compound XAV939 relative to the vehicle (DMSO), plotted on the *y*-axis, versus the percentage competition with the inactive compound LDW643 relative to DMSO, plotted on the *x*-axis. The blue border lines on each axis signify the 2 s.d. from the average competition value across all identified proteins with >3 spectra, which is indicated by the middle blue line. All proteins that are specifically competed with the active compound are highlighted in red. **b**, Immunoblot analysis for TNKS1/2, PARP1 and PARP2 on lysates from a compound competition experiment. **c**, Cy5-conjugated XAV939 directly binds the PARP domain of TNKS1 and TNKS2 with high affinity. Raw millipolarization (mP) data were analysed with a one-site total binding saturation algorithm.

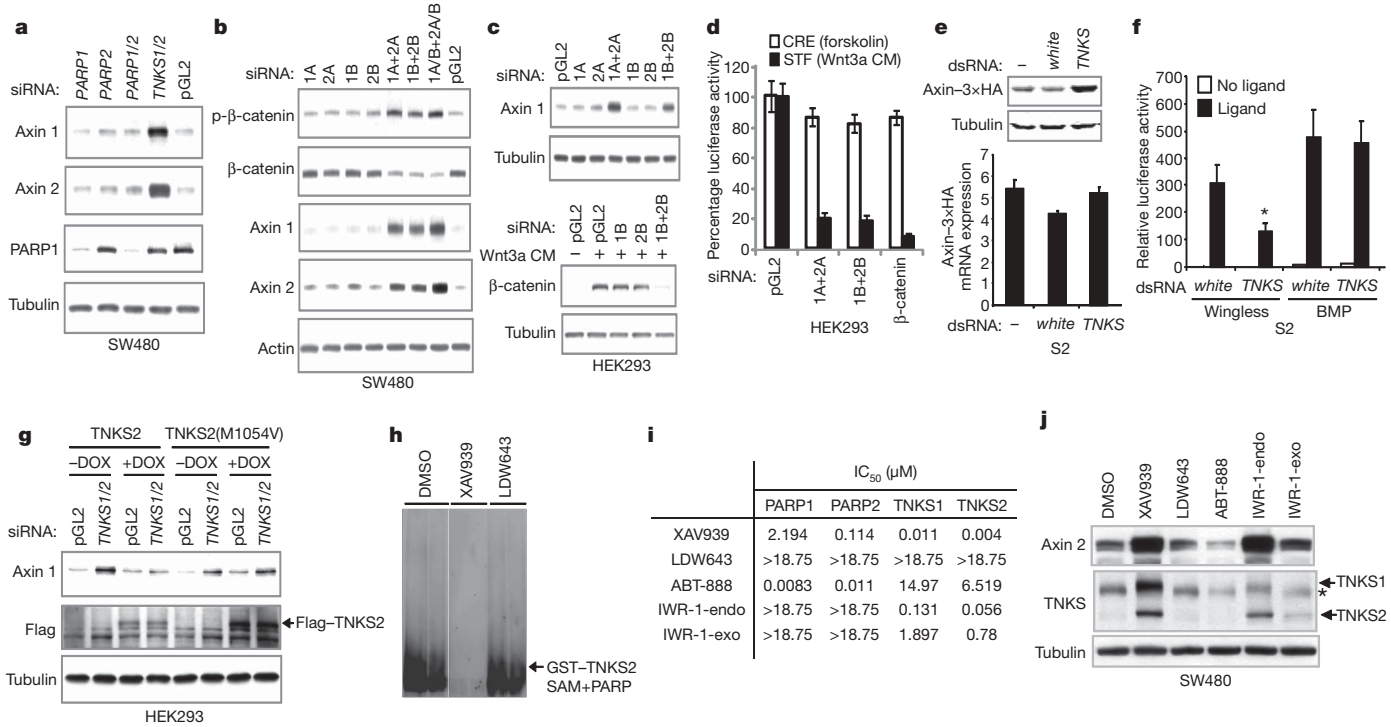

Figure 3 | Tankyrase modulates axin protein levels. **a**, **b**, Simultaneous depletion of TNKS1 and TNKS2 phenocopies XAV939 by increasing axin protein levels and decreasing β-catenin protein levels in SW480 cells. For both *TNKS1* and *TNKS2*, two independent siRNAs were generated from unique target sequences, labelled A and B (1A, 2A, 1B and 2B). **c**, Co-depletion of TNKS1 and TNKS2 increases the protein level of axin 1 (upper panel) and blocks Wnt3a-induced β-catenin accumulation (lower panel) in HEK293 cells. **d**, Co-depletion of TNKS1 and TNKS2 inhibits STF reporter, but not CRE reporter, in HEK293 cells ($n = 4$). **e**, Knockdown of TNKS increases the protein level (upper panel), but not the mRNA level (lower panel), of haemagglutinin-conjugated *Drosophila* axin (Axin–3×HA) in *Drosophila* S2 cells. dsRNA against *white* was used as control ($n = 4$). **f**, Depletion of TNKS specifically inhibits Wnt reporter (LEF–Luc), but not BMP reporter (BRE–Luc), in S2 cells ($^*P < 0.001$, $n = 4$). **g**, Doxycycline (DOX)-induced expression of wild-type TNKS2, but not catalytically inactive mutant TNKS2(M1054V), rescues *TNKS1/2* siRNA-induced accumulation of axin 1 in HEK293 cells. **h**, XAV939 inhibits auto-PARsylation of TNKS2. Recombinant TNKS2 protein used in this experiment contains the sterile alpha motif (SAM) domain and the PARP domain. **i**, Compound activity in PARP1/2 and TNKS1/2 biochemical assays. **j**, Effects of compounds (5 μM, 24 h) on the protein levels of axin 2 and TNKS1/2 in SW480 cells. A background band that migrated right below the TNKS1 band is indicated by an asterisk.

TNKS2 (Fig. 3i and Supplementary Fig. 3i), did not affect the protein levels of axin and TNKS (Fig. 3j). Collectively, these results indicate that TNKS1 and TNKS2 are the cellular efficacy targets of XAV939.

Using additional siRNAs, we further demonstrated that co-depletion of TNKS1 and TNKS2 increases β-catenin phosphorylation, decreases β-catenin abundance, and inhibits the transcription of β-catenin target genes in SW480 cells (Fig. 3b and Supplementary Fig. 3c, d). Notably, depletion of TNKS1 or TNKS2 alone did not increase axin 1/2 protein levels (Fig. 3b), indicating that TNKS1 and TNKS2 function redundantly in regulating axin protein levels. Co-depletion of TNKS1 and TNKS2 also phenocopied the pharmacological effect of XAV939 in HEK293 and DLD-1 cells (Fig. 3c, d and Supplementary Fig. 3e). In addition, combined XAV939 and *TNKS1/2* siRNA treatment increased axin protein levels even further (Supplementary Fig. 3f).

We examined whether regulation of axin and Wnt signalling by TNKS is evolutionarily conserved. We found that a double-stranded RNA (dsRNA) targeting *Drosophila TNKS* increased protein levels, but not mRNA levels, of exogenously expressed *Drosophila* axin in S2 cells (Fig. 3e and Supplementary Fig. 3g), and specifically inhibited a Wnt reporter ($P < 0.001$) (Fig. 3f). We also showed that treatment of zebrafish embryos with XAV939, but not its inactive analogue LDW643, significantly decreased the signal from a β-catenin/LEF1 reporter (TOP–GFP; green fluorescent protein) (Supplementary Fig. 4a) and inhibited the mRNA expression of the β-catenin target gene *axin2* (Supplementary Fig. 4c). Furthermore, concomitant knockdown of two zebrafish TNKS genes (*tnks1a* and *tnks1b*) with morpholinos specifically decreased TOP–GFP expression (Supplementary Fig. 4b). Together, these findings indicate that the regulatory function of TNKS in Wnt signalling is evolutionarily conserved.

Wnt signalling is required for regenerative processes in adult zebrafish, including fin regeneration[15,16]. *Inks* genes are expressed in caudal fin tissue, and no transcriptional changes are detectable after injury (Supplementary Fig. 4d, panel iii). XAV939, but not LDW643, inhibited fin regeneration (Supplementary Fig. 4d, panels i and ii) and Wnt-dependent activation of *axin2* transcription (Supplementary Fig. 4d, panel iii). This phenotype is remarkably similar to what was observed for IWR-1, an axin stabilizer recently identified[17], which we have found to also inhibit TNKS (as described in detail below). The fact that two structurally unrelated TNKS inhibitors block Wnt-dependent fin regeneration indicates that TNKS inhibition can antagonize Wnt signalling *in vivo*. However, we did not observe obvious early developmental defects associated with Wnt inhibition. Given that axin accumulation requires several hours, it is possible that the kinetics of axin stabilization are too slow to have an impact on early developmental phenotypes in this model system. Alternatively, TNKS function in Wnt pathway modulation may be cell-type- or organ-specific (for example, tail fin).

TNKS1 and TNKS2 modify their substrates through the addition of several ADP-ribose units, referred to as poly-ADP-ribosylation (PARsylation)[18]. To determine whether the PARsylation activity of TNKS is essential for regulating axin protein levels, we performed siRNA-rescue experiments. In transient transfection experiments, TNKS overexpression at high levels induces β-catenin stabilization in a PARP-domain-independent fashion. However, this is an overexpression artefact probably mediated by sequestration of endogenous axin by overexpressed TNKS (see Supplementary Fig. 6 for detailed discussion). We therefore used lentiviral transduction at a low multiplicity of infection for the rescue experiments, in which the

expression of TNKS is markedly lower than in the transient transfection experiments (data not shown). Doxycycline-induced expression of wild-type TNKS2, but not the catalytically inactive TNKS2(M1054V) mutant[19], rescued the effect of *TNKS1/2* siRNAs on axin 1 protein expression (Fig. 3g). Similar results were obtained with TNKS1 (Supplementary Fig. 3h). These data indicate that the catalytic activity of both tankyrases is required for the regulation of axin protein levels. Consistent with this finding, we showed that XAV939, but not LDW643, inhibits auto-PARsylation of TNKS2 *in vitro* (Fig. 3h). In biochemical activity assays, XAV939 strongly inhibited TNKS1 and TNKS2, with half-maximal inhibitory concentration values of 0.011 and 0.004 μM, respectively, but displayed much weaker effects on PARP1 and PARP2 (Fig. 3i). Auto-PARsylation of TNKS has been reported to promote its own degradation through the ubiquitin-proteasome pathway[20]. We found that XAV939 treatment led to a significant increase in TNKS protein levels (Fig. 3j), indicating that XAV939 also inhibits TNKS auto-PARsylation *in vivo*.

A recent study described two compound series (IWR-1, -2, and IWR-3, -4, -5) that increase axin protein levels and inhibit Wnt signalling[17]. It was shown that IWR-1-endo (also referred to as IWR-1) increased axin protein levels, whereas its close analogue IWR-1-exo had much weaker activity. Although the authors suggested that IWR-1 might stabilize axin by binding to a region in the carboxy-terminal half of axin, we examined whether IWR-1 compounds may in fact stabilize axin by inhibiting TNKS. Notably, IWR-1-endo strongly inhibited TNKS1 and TNKS2 in biochemical assays, with IWR-1-exo being approximately tenfold less active (Fig. 3i and Supplementary Fig. 3i), consistent with their potency in axin stabilization assays (Fig. 3j). In contrast, neither of these two compounds inhibited PARP1/2 (Fig. 3i). Consistent with the activity of IWR-1-endo in TNKS1/2 biochemical assays, IWR-1-endo, but not IWR-1-exo, significantly stabilized endogenous TNKS1, TNKS2 and axin 2 (Fig. 3j and Supplementary Fig. 3j), indicating that IWR-1-endo inhibited auto-PARsylation of TNKS *in vivo*. These results indicate that IWR-1-endo stabilizes axin at least in part through TNKS inhibition. Together, our data demonstrate that the PARsylation activity of TNKS1/2, but not PARP1/2, is required for the regulation of axin protein levels.

TNKS interacts with axin to regulate axin levels

We next explored how TNKS regulates axin protein levels. Using co-immunoprecipitation experiments, we found that endogenous TNKS1 and TNKS2 associate with axin 2 in SW480 cells (Fig. 4a). In addition, we detected a strong interaction between axin 1/2 and TNKS1/2 in the yeast two-hybrid assay (Fig. 4b and data not shown). The ankyrin repeat domain of TNKS1 was required and sufficient for the interaction with axin 1 (Supplementary Fig. 6a). Strikingly, a small amino-terminal region of axin 1 (amino acids 19–30), which encompasses the most conserved stretch of amino acids within axin (Fig. 4c), was both required and sufficient to interact with TNKS1 (Fig. 4b). The specific interaction of axin 1 with TNKS1 through this domain, which we named tankyrase-binding domain (TBD), was further substantiated by glutathione *S*-transferase (GST) pull-down and co-immunoprecipitation assays (Fig. 4d, e).

We next assessed the functional consequences of disrupting the physical interaction between axin and TNKS. If binding between axin and TNKS promoted axin degradation, deletion of the TBD should result in the stabilization of axin. Indeed, whereas cells expressing wild-type GFP–axin 1 demonstrated low basal protein levels that were strongly increased in response to XAV939 treatment, cells expressing GFP–axin 1(Δ19–30) already exhibited high basal protein levels that did not further respond to compound treatment (Fig. 4f and Supplementary Fig. 5). Importantly, restoring the TNKS1–axin 1 interaction by fusing the heterologous TNKS binding domain of either IRAP (insulin-regulated aminopeptidase, also known as LNPEP) or TRF1 (telomeric repeat binding factor, also known as TERF1) to GFP–axin 1(Δ19–30) fully restored its response to XAV939 (Fig. 4f). We further hypothesized that overexpression of the N-terminal domain of axin may compete with endogenous axin for the binding of TNKS and thus stabilize axin. Indeed, overexpression of GFP–axin 1N (amino acids 1–87), but not the mutant with the

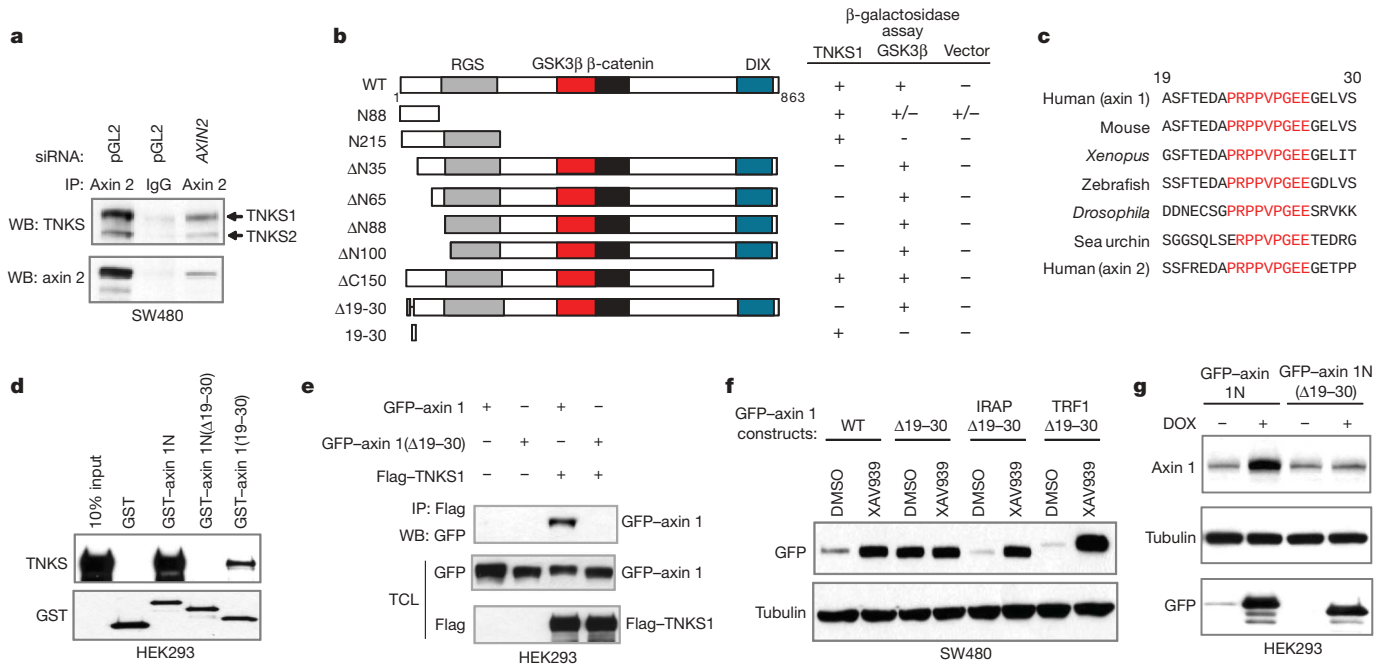

Figure 4 | Tankyrase physically and functionally interacts with axin. a, Co-immunoprecipitation of endogenous axin 2 and TNKS in SW480 cells. **b**, Binding between axin 1 fragments and TNKS1 in the yeast two-hybrid assay (+, strong binding; +/−, weak binding; −, no binding). The N88 fragment retains partial self-activation activity. **c**, The TBDs of axin proteins are evolutionarily conserved. Highly conserved amino acid residues are depicted in red. **d**, The N-terminal fragment of axin 1 (amino acids 1–87) binds to TNKS1 in a GST pull-down assay. **e**, The TBD is required for the interaction between axin 1 and TNKS in a co-immunoprecipitation assay. **f**, The TBD is required for XAV939-induced axin 1 protein accumulation in SW480 cells. The expression of GFP–axin 1 was under the control of the metallothionein promoter to ensure low transcription. **g**, DOX-induced overexpression of GFP–axin 1N (amino acids 1–87) leads to accumulation of endogenous axin 1 in HEK293 cells.

deleted TBD, substantially increased endogenous axin 1 protein levels while not affecting its mRNA expression (Fig. 4g and data not shown). Together, these findings demonstrate that the physical interaction between axin and TNKS, which is mediated by the evolutionarily conserved TBD, is critical for regulating axin protein levels.

Axin is degraded through PARsylation and ubiquitination

The increase in axin protein levels in response to XAV939 treatment could be due to modulation of translation or protein stability. Consistent with the latter possibility, XAV939 treatment prolonged the half-life of endogenous axin 2 in SW480 cells (Fig. 5a). The degradation of axin is probably mediated by the ubiquitin-proteasome pathway, because the polyubiquitination of axin 1 increased significantly after addition of the proteasome inhibitor MG132 (Fig. 5b). In contrast, co-treatment of XAV939 with MG132 significantly diminished axin 1 and axin 2 polyubiquitination (Fig. 5b and Supplementary Fig. 7a), indicating that XAV939 may stabilize axin by preventing its polyubiquitination.

Auto-PARsylation of TNKS or TNKS-mediated TRF1 PARsylation leads to ubiquitination and degradation of TNKS or TRF1, respectively[20,21]. Together with our findings, this raised the possibility that axin degradation may be facilitated through direct PARsylation by TNKS. Indeed, TNKS2 was able to PARsylate an axin 1 fragment (amino acids 1–280) containing the TBD *in vitro* (Fig. 5c), which was completely inhibited by XAV939 treatment (Fig. 5c). Using an antibody that specifically recognizes the PAR modification, we also observed that exogenously expressed GFP–axin 1 was PARsylated in cells (Fig. 5d). In addition, the PARsylation signal was strongly reduced in the presence of XAV939 (Fig. 5d), indicating that axin PARsylation is mediated by TNKS *in vivo*. To enhance the detection of endogenous axin 2 ubiquitination and PARsylation, we pretreated cells with XAV939 to increase endogenous axin 2 levels. Axin 2 was rapidly degraded within 1 h after XAV939 was washed off (Fig. 5e). As expected, treatment of MG132 blocked axin 2 degradation and strongly increased its polyubiquitination (Fig. 5e and Supplementary Fig. 7b). Treatment with XAV939 and MG132, however, completely blocked the ubiquitination of axin 2 (Fig. 5e and Supplementary Fig. 7b). Interestingly, an anti-PAR antibody reactive signal that co-migrated with axin 2 was detected when cells were treated with MG132 alone and disappeared when cells were also treated with XAV939 (Fig. 5e). Together, these findings are consistent with the hypothesis that TNKS promotes the ubiquitination and degradation of axin, which may be mediated, at least in part, through the direct PARsylation of axin.

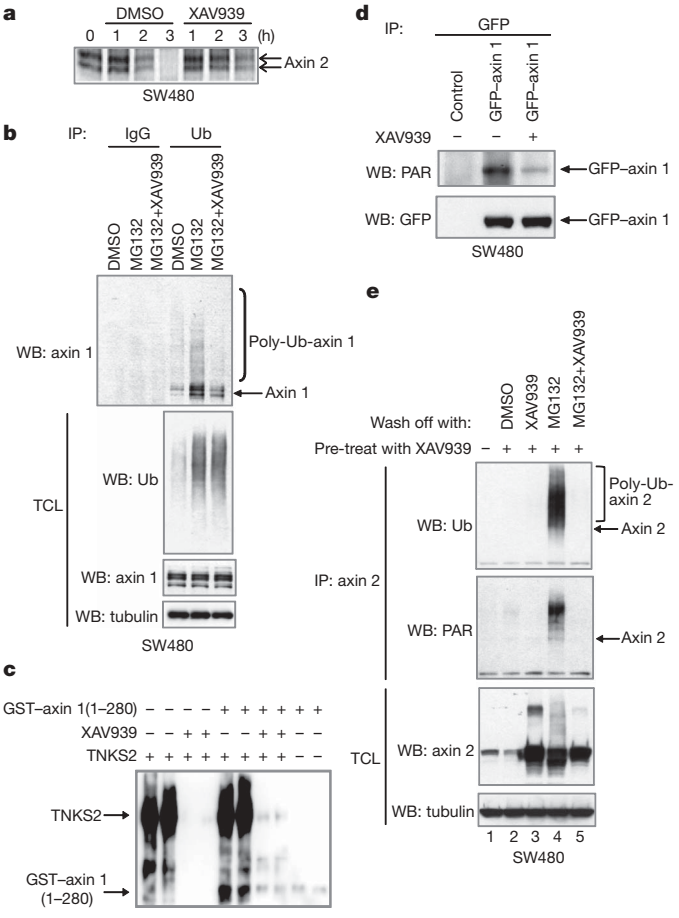

Figure 5 | XAV939 stabilizes axin protein and inhibits ubiquitination of axin. **a**, XAV939 (1 μM) stabilizes axin 2 in SW480 cells as indicated by a pulse-chase analysis. **b**, Ubiquitination of axin is inhibited by XAV939 (1 μM). The position of axin 1 is labelled with an arrow. Slow-migrating polyubiquitinated axin 1 conjugates are indicated. **c**, *In vitro* PARsylation of GST–axin 1 (amino acids 1–280) by TNKS2. **d**, XAV939 (1 μM, 6 h) inhibits *in vivo* PARsylation of axin 1. **e**, Post-translational modification of axin 2 in a compound wash-off experiment. SW480 cells pretreated with XAV939 were washed and incubated with medium supplemented with the indicated compound for 1 h, and analysed by the immunoprecipitation assay. The position of axin 2 is indicated by the arrows. IP, immunoprecipitation; TCL, total cell lysates.

XAV939 inhibits growth of DLD-1 cancer cells

Because XAV939 inhibited β-catenin signalling even in APC-deficient cells, we examined whether this compound could inhibit the proliferation of APC-deficient colorectal cancer cells using β-catenin-dependent DLD-1 cells and β-catenin-independent RKO cells (Supplementary Fig. 8a). Under low serum growth conditions, XAV939, but not the inactive analogue LDW643, significantly inhibited colony formation of DLD-1 cells (Fig. 6a). Importantly, XAV939 did not affect colony formation in RKO cells (Fig. 6b).

TNKS1 was proposed to be required for the resolution of sister telomere association or assembly of bipolar spindles, and *TNKS1* knockdown was reported to cause strong mitotic arrest[22,23]. However, using XAV939 treatment or individual/combinatorial *TNKS1/TNKS2* siRNA knockdown, we did not observe any overt mitotic arrest phenotype (Supplementary Fig. 8b and data not shown), demonstrating that XAV939 does not inhibit the proliferation of DLD-1 cells through an antimitotic function.

If the antiproliferative effect of XAV939 on DLD-1 cells was instead mediated by an increase in axin protein levels, knockdown of *AXIN1/2* may rescue the growth inhibitory effects of compound treatment. Indeed, siRNA-mediated depletion of axin 1 and axin 2 proteins completely abolished the antiproliferative effect of XAV939 (Fig. 6c), indicating that the growth inhibitory effects of XAV939 in DLD-1 cells are due to axin-dependent inhibition of Wnt signalling.

Discussion

Despite the fact that the Wnt pathway is an attractive target for anticancer therapy, there are few druggable targets in this pathway to generate small molecule Wnt inhibitors. Using a chemical genetics approach, we have discovered tankyrases as novel targets for Wnt inhibition and described a novel mechanism to promote β-catenin degradation through inhibition of tankyrases and stabilization of axin (Supplementary Fig. 9). This finding may pave the way for mechanism-based treatments of Wnt-dependent cancers.

Our data indicate that tankyrases are physiological regulators of axin protein homeostasis and Wnt signalling. Although the precise mechanistic details remain unclear, tankyrases seem to promote the ubiquitination of axin, possibly through direct PARsylation of axin. Notably, TNKS-mediated PARsylation seems to also stimulate ubiquitin-mediated proteolysis of TRF1 and TNKS itself[20,21]. These findings indicate that coupling of these biochemical processes may be a more general regulatory mechanism, akin to the widespread occurrence of phosphodegrons that couple phosphorylation to ubiquitination[24,25].

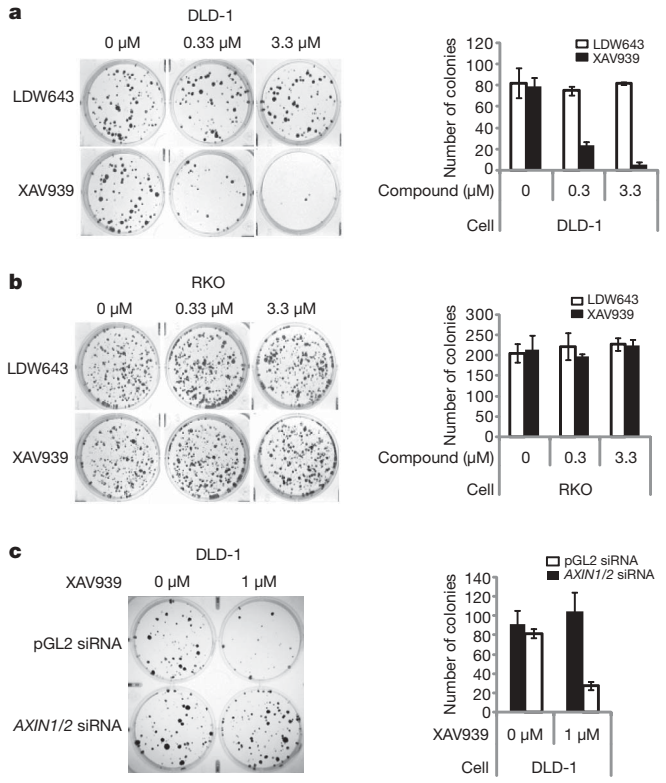

Figure 6 | XAV939 inhibits DLD-1 colony formation in an axin-dependent manner. a, **b**, XAV939 inhibits colony formation of DLD-1, but not RKO, cells. DLD-1 and RKO cells were seeded and grown in 0.5% serum medium containing the indicated compounds ($n = 3$). The number of colonies in each well was counted. **c**, The effect of XAV939 on DLD-1 colony formation is axin-dependent. DLD-1 cells were transfected with siRNAs against *AXIN1* and *AXIN2* or control pGL2 siRNA, and tested in the colony formation assay ($n = 3$).

Tnks1$^{-/-}$ and *Tnks2*$^{-/-}$ mice are largely normal and double knockout of *Tnks1/2* causes early embryonic lethality, indicating their redundancy in mouse development[26,27]. Conditional knockout of both *Tnks1* and *Tnks2* will be important to understand the role of tankyrases in regulation of Wnt signalling in tissue homeostasis and disease.

Axin is a concentration-limiting factor in the β-catenin degradation complex[7,8]. Our study further highlights the importance of axin as a key regulatory node in the Wnt signalling cascade. We speculate that axin may function more generally as a signal 'integrator' and that other proteins/pathways may modulate Wnt pathway activity by impinging on this key regulatory node. Further investigation of the molecular mechanisms that regulate axin protein and their potential deregulation in disease conditions is likely to provide additional avenues for treating Wnt-dependent cancers and other Wnt-related diseases.

METHODS SUMMARY

Compound affinity purification and mass spectrometry analysis. Compound affinity purification, mass spectrometry and data analysis were performed essentially as previously described[28]. A derivatized, bioactive analogue LDW639 with a primary amine group was coupled to NHS (*N*-hydroxysuccinimide)-activated Sepharose 4 beads. HEK293 cells were homogenized in lysis buffer (50 mM Tris-HCl, pH 7.5, 5% glycerol, 1.5 mM $MgCl_2$, 150 mM NaCl, 20 mM NaF, 1 mM Na_3VO_4, 1 mM dithiothreitol, 5 μM calyculin A, 0.8% Igepal-CA630 and a protease inhibitor cocktail). Cell lysates were pre-incubated with 20 μM XAV939, LDW643 or DMSO for 30 min, and incubated with LDW639-matrix for another 60 min. After extensive washes, bound material was eluted and resolved by SDS–polyacrylamide gel electrophoresis. Gel lanes were cut into slices across the full separation range and subjected to in-gel tryptic digestion, followed by iTRAQ labelling (Applied Biosystems). Peptides extracted from DMSO-treated samples were labelled with iTRAQ reagent 116 and combined with extracts of compound-treated samples labelled with iTRAQ reagents 114 and 115, respectively. Liquid chromatography–tandem mass spectrometry was done using an Eksigent 1D+ HPLC system coupled to a LTQ Orbitrap mass spectrometer (Thermo-Finnigan). Tandem mass spectra were generated using pulsed-Q dissociation, enabling detection of iTRAQ reporter ions[29]. Peptide mass and fragmentation data were used to query an in-house curated version of the IPI database using Mascot (Matrix Science). Protein identifications were validated using a decoy database. iTRAQ reporter ion-based quantification was performed with software developed in-house.

Received 7 May; accepted 30 July 2009.
Published online 16 September 2009.

1. Clevers, H. Wnt/β-catenin signaling in development and disease. *Cell* **127,** 469–480 (2006).
2. Polakis, P. The many ways of Wnt in cancer. *Curr. Opin. Genet. Dev.* **17,** 45–51 (2007).
3. Barker, N. & Clevers, H. Mining the Wnt pathway for cancer therapeutics. *Nature Rev. Drug Discov.* **5,** 997–1014 (2006).
4. Miyaki, M. *et al.* Characteristics of somatic mutation of the adenomatous polyposis coli gene in colorectal tumors. *Cancer Res.* **54,** 3011–3020 (1994).
5. Mori, Y. *et al.* Somatic mutations of the *APC* gene in colorectal tumors: mutation cluster region in the *APC* gene. *Hum. Mol. Genet.* **1,** 229–233 (1992).
6. Powell, S. M. *et al.* APC mutations occur early during colorectal tumorigenesis. *Nature* **359,** 235–237 (1992).
7. Salic, A., Lee, E., Mayer, L. & Kirschner, M. W. Control of β-catenin stability: reconstitution of the cytoplasmic steps of the Wnt pathway in *Xenopus* egg extracts. *Mol. Cell* **5,** 523–532 (2000).
8. Lee, E., Salic, A., Kruger, R., Heinrich, R. & Kirschner, M. W. The roles of APC and axin derived from experimental and theoretical analysis of the Wnt pathway. *PLoS Biol.* **1,** E10 (2003).
9. Behrens, J. *et al.* Functional interaction of an axin homolog, conductin, with β-catenin, APC, and GSK3β. *Science* **280,** 596–599 (1998).
10. Kishida, M. *et al.* Axin prevents Wnt-3a-induced accumulation of β-catenin. *Oncogene* **18,** 979–985 (1999).
11. Hart, M. J., de los Santos, R., Albert, I. N., Rubinfeld, B. & Polakis, P. Downregulation of β-catenin by human axin and its association with the APC tumor suppressor, β-catenin and GSK3β. *Curr. Biol.* **8,** 573–581 (1998).
12. Leung, J. Y. *et al.* Activation of *AXIN2* expression by β-catenin-T cell factor. A feedback repressor pathway regulating Wnt signaling. *J. Biol. Chem.* **277,** 21657–21665 (2002).
13. Willert, K., Shibamoto, S. & Nusse, R. Wnt-induced dephosphorylation of axin releases β-catenin from the axin complex. *Genes Dev.* **13,** 1768–1773 (1999).
14. Donawho, C. K. *et al.* ABT-888, an orally active poly(ADP-ribose) polymerase inhibitor that potentiates DNA-damaging agents in preclinical tumor models. *Clin. Cancer Res.* **13,** 2728–2737 (2007).
15. Poss, K. D., Shen, J. & Keating, M. T. Induction of *lef1* during zebrafish fin regeneration. *Dev. Dyn.* **219,** 282–286 (2000).
16. Stoick-Cooper, C. L. *et al.* Distinct Wnt signaling pathways have opposing roles in appendage regeneration. *Development* **134,** 479–489 (2007).
17. Chen, B. *et al.* Small molecule-mediated disruption of Wnt-dependent signaling in tissue regeneration and cancer. *Nature Chem. Biol.* **5,** 100–107 (2009).
18. Hsiao, S. J. & Smith, S. Tankyrase function at telomeres, spindle poles, and beyond. *Biochimie* **90,** 83–92 (2008).
19. Sbodio, J. I., Lodish, H. F. & Chi, N. W. Tankyrase-2 oligomerizes with tankyrase-1 and binds to both TRF1 (telomere-repeat-binding factor 1) and IRAP (insulin-responsive aminopeptidase). *Biochem. J.* **361,** 451–459 (2002).
20. Yeh, T.-Y. *et al.* Tankyrase recruitment to the lateral membrane in polarized epithelial cells: regulation by cell–cell contact and protein poly(ADP-ribosyl)ation. *Biochem. J.* **399,** 415–425 (2006).
21. Chang, W., Dynek, J. N. & Smith, S. TRF1 is degraded by ubiquitin-mediated proteolysis after release from telomeres. *Genes Dev.* **17,** 1328–1333 (2003).
22. Chang, P., Coughlin, M. & Mitchison, T. J. Tankyrase-1 polymerization of poly(ADP-ribose) is required for spindle structure and function. *Nature Cell Biol.* **7,** 1133–1139 (2005).
23. Dynek, J. N. & Smith, S. Resolution of sister telomere association is required for progression through mitosis. *Science* **304,** 97–100 (2004).
24. Winston, J. T. *et al.* The SCF$^{β\text{-}TRCP}$-ubiquitin ligase complex associates specifically with phosphorylated destruction motifs in IκBα and β-catenin and stimulates IκBα ubiquitination *in vitro*. *Genes Dev.* **13,** 270–283 (1999).
25. Koepp, D. M. *et al.* Phosphorylation-dependent ubiquitination of cyclin E by the SCF^{Fbw7} ubiquitin ligase. *Science* **294,** 173–177 (2001).
26. Hsiao, S. J., Poitras, M. F., Cook, B. D., Liu, Y. & Smith, S. Tankyrase 2 poly(ADP-ribose) polymerase domain-deleted mice exhibit growth defects but have normal telomere length and capping. *Mol. Cell. Biol.* **26,** 2044–2054 (2006).
27. Chiang, Y. J. *et al.* Tankyrase 1 and tankyrase 2 are essential but redundant for mouse embryonic development. *PLoS ONE* **3,** e2639 (2008).
28. Bantscheff, M. *et al.* Quantitative chemical proteomics reveals mechanisms of action of clinical ABL kinase inhibitors. *Nature Biotechnol.* **25,** 1035–1044 (2007).
29. Bantscheff, M. *et al.* Robust and sensitive iTRAQ quantification on an LTQ Orbitrap mass spectrometer. *Mol. Cell. Proteomics* **7,** 1702–1713 (2008).

Supplementary Information is linked to the online version of the paper at www.nature.com/nature.

Acknowledgements We thank D. Patel, F. Harbinski, J. Leighton-Davies, R. de Beaumont, X. Xiang, K. Bean, C. Xin, S. Zhao, B. Zhang and M. Xu for technical assistance, G. Wussler, H. Urquiza and W. Dai for zebrafish maintenance, and I. Cornella Taracido, S. Cleaver, A. Hernandez and Y. Ben-Neriah for comments and advice. In addition we are indebted to B. Kuster, J. Rick, M. Raida and A. Scholten for continued support and discussion.

Author Contributions S.-M.A.H., A.C., F.St., G.A.M., E.W., V.M., S.F., C.Lu, D.C., M.W.K., C.Le., P.M.F., J.A.T., T.B., J.A.P., A.B. and F.C. conceived and designed the study. S.-M.A.H., Y.M.M., S.L., A.C., F.St., G.A.M., O.C., E.W., Y.Z., S.W., M.H., X.S., C.W., C.M., A.F., R.T., F.Se., W.S., H.C., M.Sh., C.R., M.Sc., J.S., S.G., A.B. and F.C. designed and implemented experiments. S.-M.A.H., F.St., A.B., Y.M.M. and F.C. wrote the paper.

Author Information Reprints and permissions information is available at www.nature.com/reprints. Correspondence and requests for materials should be addressed to F.C. (feng.cong@novartis.com).